

MOTIVATION AND DATA

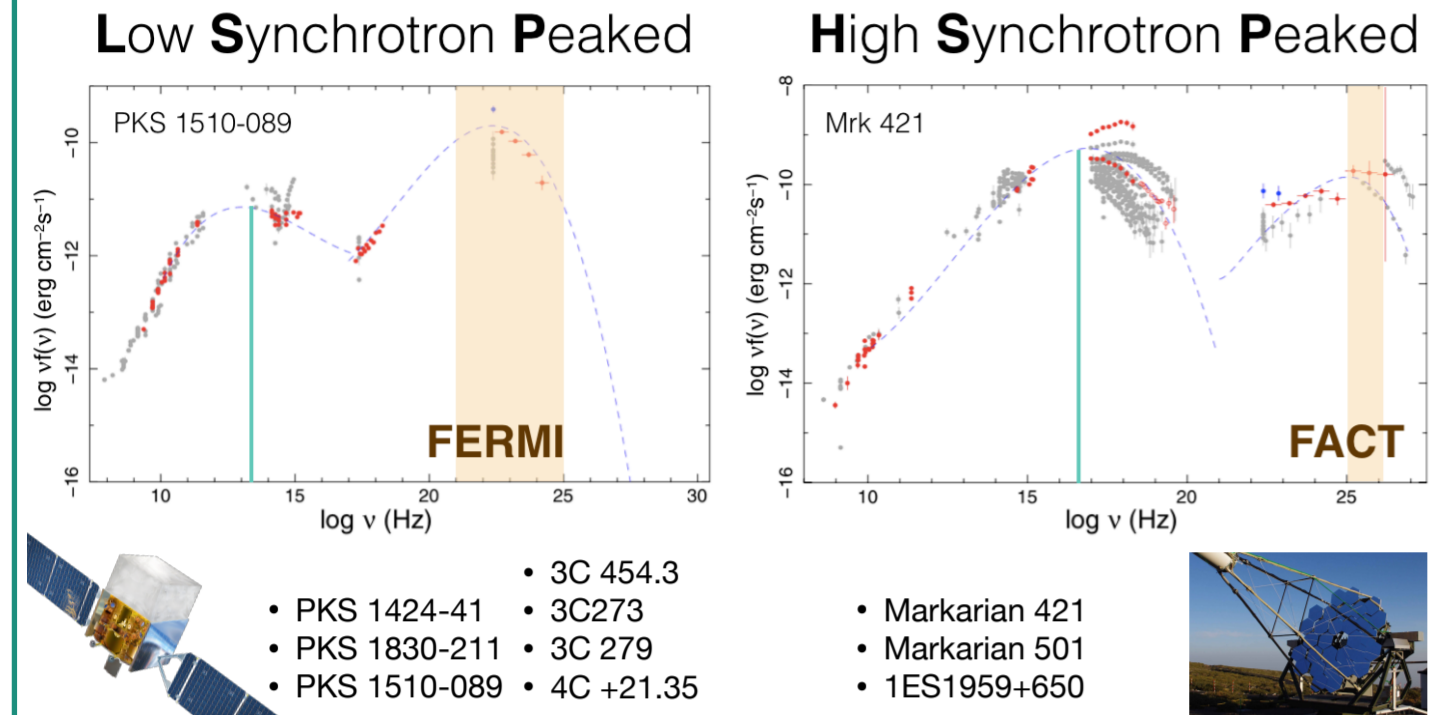


Figure 1: Based on the peak position of the low energy hump (cyan line) in the spectral energy distribution, blazars can be classified as low- and high-synchrotron peaked objects (LSP and HSP), as shown for PKS 1510-089 and Mrk 421, respectively. The intrinsic difference between these classes as well as the processes responsible for the high-energy hump remain uncertain. Thus, we analyze the high-energy variability with *Fermi*-LAT and FACT (bottom left and right) which cover the respective high-energy hump for the brightest LSP and HSP sources as listed below the SEDs.

Data analysis *Fermi*-LAT:

- time: 2008-08-05 to 2020-12-31
- energy: 100 MeV to 300 GeV
- only flux bins with $TS > 4$ and flux error $<$ flux
- standard analysis (see proceedings article)

Data analysis FACT:

- time: 2011-11-15 to 2020-01-23
- energy: above 300 GeV
- light curve divided into chunks (seasonal gaps)
- standard analysis (see proceedings article)

CONCLUSIONS

- Daily binned GeV (*Fermi*-LAT) as well as TeV (FACT) flares determined with HOP algorithm result in:
 - Large fraction of single block flares \rightarrow suggests flux variations take place on intra-day timescales
 - No preferred asymmetry for flares with more than one block
- High-energy flux fluctuations could, for instance, be produced by one or several plasmoids moving along the jet [3]
- Ornstein-Uhlenbeck parameter extraction indicates that amplitude of random fluctuations differs for the samples considered

KEYWORDS

(very) high-energy γ -ray, blazars, variability, flare asymmetry, time series analysis, stochastic (Ornstein-Uhlenbeck) process

VARIABILITY ANALYSIS

- Characterize flares with the HOP algorithm as shown in Fig. 2, following [1]

1. Apply the Bayesian block algorithm
2. Peak time = center of local maximum
3. Subsequently lower blocks belong to peak (watershed method)
4. Define start and end time of a flare; similar results (Fig. 3 and Fig. 4) for either method
 - (a) *baseline*: Determined by flux exceeding/dropping under certain flux level (e.g. quiescent background)
 - (b) *half*: Divide valley blocks in half
 - (c) *sharp*: Neglect valley blocks
 - (d) *flip*: Extrapolate slope of flare by flipping length of adjacent block onto valley block \rightarrow this work

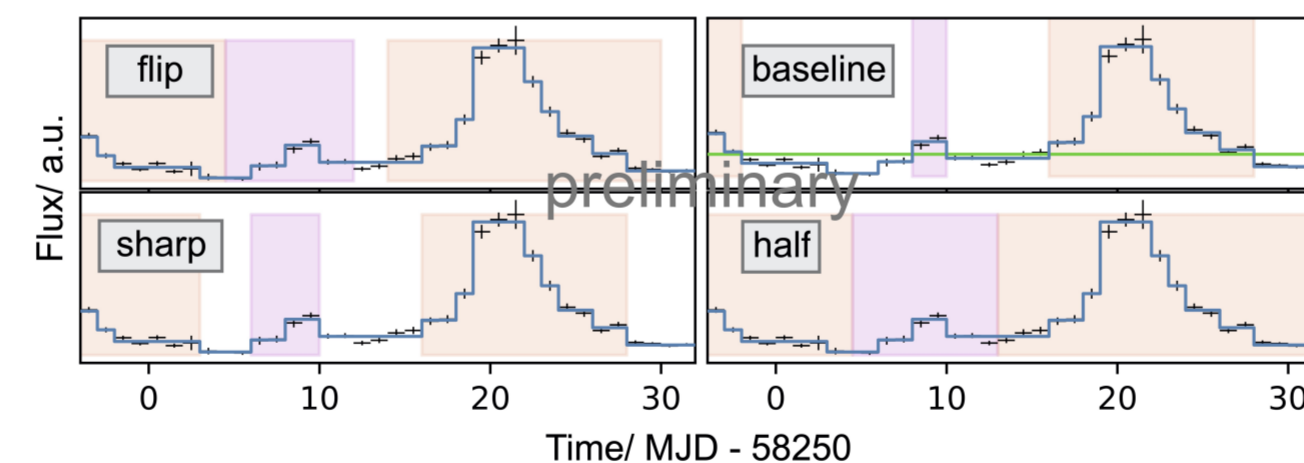


Figure 2: Based on Bayesian blocks (blue) and corresponding method, we define flares (orange and purple) in the daily binned light curves (here: *Fermi*-LAT, 3C 279).

- Extract OU parameters of each light curve [2] Assume flux variations are correlated noise parametrized by a first order auto-regressive process; the discrete OU process (see Eq. 5e in [2])

$$u_{T+1} = u_T + \theta \Delta t (\mu - u_T) + \sigma \sqrt{\Delta t} \mathcal{N}_T \quad (1)$$

- \rightarrow μ = mean revision level, θ = mean revision rate
- \rightarrow White noise implemented with independent draws from normal distribution $\mathcal{N}(m = 0, \sigma^2)$
- \rightarrow Value of the time series u_T is logarithm of flux

RESULTS

47% (*Fermi*-LAT) and 48% (FACT) of all flares consist of a single block indicating shorter variability that is not resolved in daily binning. We exclude these flares and compute for all remaining flares the asymmetry measure

$$A = \frac{t_{\text{rise}} - t_{\text{decay}}}{t_{\text{rise}} + t_{\text{decay}}} \quad (2)$$

with t_{rise} and t_{decay} determined by the start, peak, and end time. The probability density for A is shown in Fig. 3.

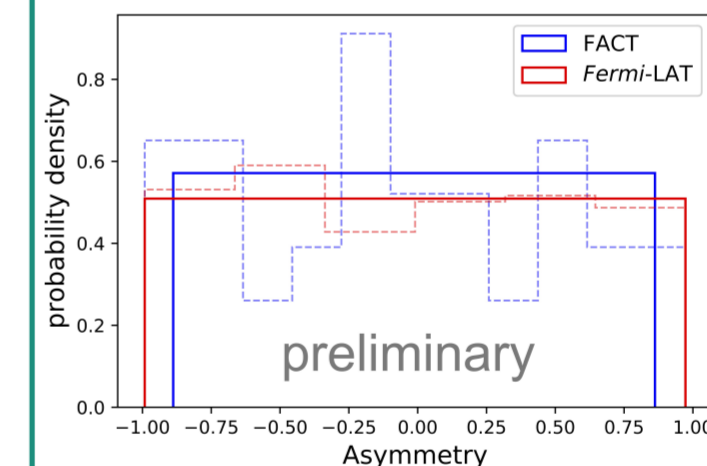


Figure 3: Probability density for asymmetry measures of *Fermi*-LAT and FACT flares in constant (dashed line) and Bayesian binning (solid line).

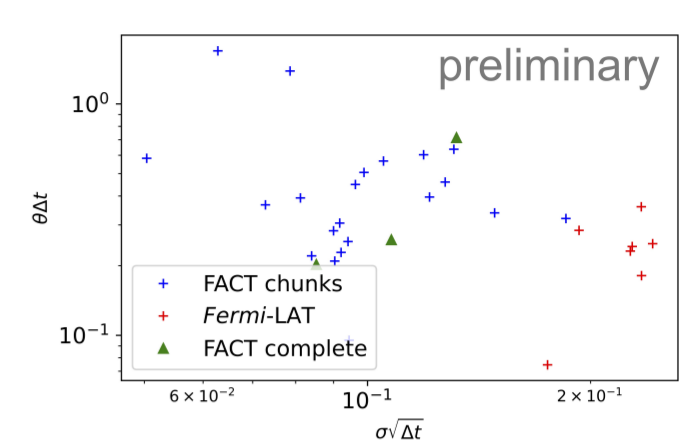


Figure 4: Scatter plot of the extracted OU parameters σ and θ for the *Fermi*-LAT light curves and FACT chunks (as analyzed before) as well as the complete FACT light curves.

We obtain two statistically equivalent, flat distributions, ranging from -1 to $+1$, meaning that each kind of asymmetry occurs to a comparable degree and we do not find differences between the two samples. The extracted OU parameters σ and θ are shown in Fig. 4. The former clearly differs for the LSP and HSP sources (*Fermi*-LAT and the FACT chunks/light curves, respectively).

REFERENCES

- [1] M. Meyer, J. D. Scargle and R. D. Blandford, *Characterizing the Gamma-Ray Variability of the Brightest Flat Spectrum Radio Quasars Observed with the Fermi LAT*, *ApJ* **877** (2019) 39 [1902.02291].
- [2] P. R. Burd, L. Kohlhepp, S. M. Wagner, K. Mannheim, S. Buson and J. D. Scargle, *Ornstein-Uhlenbeck parameter extraction from light curves of Fermi-LAT observed blazars*, *A&A* **645** (2021) A62 [2010.12318].
- [3] M. Meyer, M. Petropoulou and I. M. Christie, *The Observability of Plasmoid-powered γ -Ray Flares with the Fermi Large Area Telescope*, *MNRAS* **500** (2021) 40 [2012.09944].

CONTACT INFORMATION

GitHub github.com/swagner-astro

Email sarah.wagner@physik.uni-wuerzburg.de

